第 33 卷第 5 期
2017 年 5 月

无 机 化 学 学 报
CHINESE JOURNAL OF INORGANIC CHEMISTRY

Vol.33 No.5
769-778

一种同时分辨识别 Zn^{2+}和 F^-离子的双功能探针

曾 莉[1] 赵江林[2] 牟 兰[1] 曾 晞*,[1] 卫 钢*,[3] Redshaw Carl[4] 金宗文[2]

([1]贵州大学贵州省大环与超分子化学重点实验室,贵阳 550025)

([2]中国科学院深圳先进技术研究院,生物医学与健康工程研究所,微纳系统与仿生医学研究中心,深圳 518055)

([3]澳大利亚联邦科学与工业研究组织,制造业,新南威尔士州,悉尼 2070)

([4]英国赫尔大学化学系,赫尔 HU6 7RX)

摘要:由 8-甲酰基-7-羟基香豆素与碳酰肼经一步缩合反应可制得探针 **1**。研究发现,探针 **1** 对 Zn^{2+}和 F^-离子均呈现荧光增强和比率比色的高灵敏和高选择性响应,检出限低至 10^{-8} mol·L^{-1}。通过光谱、ITC、^{1}H NMR 滴定及质谱分析,详细地研究了探针与离子形成的配合物性质。在不同的介质中,探针不仅同时表现出对金属阳离子 Zn^{2+}和对阴离子 F^-的识别,而且吸收和发射波长均有显著的差异:**1**-Zn^{2+}配合物的最大吸收波长为 360 nm, 而 **1**-F^-配合物为 400 nm;**1**-Zn^{2+}配合物的荧光激发和发射波长分别为 360 和 454 nm,而 **1**-F^-配合物分别为 400 和 475 nm。此外,探针 **1** 还能应用于活体 PC3 细胞中 Zn^{2+}的荧光成像。

关键词:8-甲酰基-7-羟基香豆素; Zn^{2+}; F^-; 分辨波长; 细胞成像

中图分类号:O657 **文献标识码**:A **文章编号**:1001-4861(2017)05-0769-10

DOI:10.11862/CJIC.2017.076

A Readily Accessible Difunctional Probe: Simultaneous Recognition of Cation Zn^{2+} and Anion F^- via Distinguishable Wavelengths

ZENG Li[1] ZHAO Jiang-Lin[2] MU Lan[1] ZENG Xi*,[1] WEI Gang*,[3] Redshaw Carl[4] JIN Zongwen[2]

([1]*Key Laboratory of Macrocyclic and Supramolecular Chemistry of Guizhou Province, Guizhou University, Guiyang* 550025, *China*)

([2]*Research Center for Micro/Nano System & Bionic Medicine, Institute of Biomedical & Health Engineering, Shenzhen Institutes of Advanced Technology, Chinese Academy of Sciences, Shenzhen, Guangdong* 518055, *China*)

([3]*CSIRO Manufacturing, PO Box* 218, *NSW* 2070, *Australia*)

([4]*Department of Chemistry, University of Hull, Hull HU*6 7*RX, U.K.*)

Abstract: The probe **1** was readily prepared via condensation of 8-formyl-7-hydroxy-coumarin and carbonic dihydrazide in a one-step procedure. Probe **1** exhibited high sensitivity and selectivity towards Zn^{2+} and F^- through a "turn-on" fluorescence response and/or ratiometric colorimetric response with low detection limits of the order of 10^{-8} mol·L^{-1}. The complex behaviour was fully investigated by spectral titration, isothermal titration calorimetry, ^{1}H NMR spectroscopic titration and mass spectrometry. Interestingly, probe **1** not only recognizes the cation Zn^{2+} and the anion F^-, but can also distinguish between these two ions via the max wavelength in their UV-Vis spectra (360 nm for **1**-Zn^{2+} vs 400 nm for **1**-F^- complex) or their fluorescent spectra (λ_{ex}, λ_{em}=360, 454 nm for **1**-Zn^{2+} vs λ_{ex}, λ_{em}=400, 475 nm for **1**-F^- complex) due to their differing red-shifts. Additionally, probe **1** has been further explored in the detection of Zn^{2+} in living cells.

Keywords: 8-formyl-7-hydroxy-coumarin; Zn^{2+} and F^-; distinguishable wavelengths; living cells

收稿日期:2016-12-09。收修改稿日期:2017-02-27。

国家自然科学基金(No.21165006)、教育部"春晖计划"(No.Z2015007,Z2016008)、深圳市基础研究项目(No.JCYJ20140610151856726)、深圳市技术攻关项目(No.JSGG20141118113131546)和中国博士后自然基金(No.2015M582439)资助。

*通信联系人。E-mail:zengxi1962@163.com,gang.wei@csiro.au

Fluorescent probe assays are one of the most convenient technologies for detecting ions and molecules owing to their high sensitivity, selectivity, rapid response rates and ease of manipulation[1-7]. Together with their capacity for real-time imaging, these attributes have led to their wide adoption in the detection of biologically relevant ions[8-12]. A desirable fluorescent probe should not only be easily obtained, but should also allow for the simultaneously detection of both cations and anions with high sensitivity and selectivity. However, most reported probes are capable of only single target detection. Indeed, there are only a limited number of probes which satisfy such requirements, but most of these probes are very difficult to prepare[13-18].

Herein, we introduce a facile one step synthesis of a difunctional, ratiometric colorimetric/fluorescent probe **1**, which is derived from the condensation reaction of 7-hydroxy-8-aldehyde-coumarin and carbohydrazide. Probe **1** not only exhibits high selectivity for the Zn^{2+} cation, but also high selectivity for F^- anions over a number of other cations and anions tested herein with distinct colour changes. Furthermore, the response signal for the addition of Zn^{2+} vs F^- is easily distinguishable. This selective detection is the result of the 40 nm of wavelength differences observed in the UV-Vis absorption spectra upon addition of the Zn^{2+} cation vs the F^- anion. Hence, using probe **1** it is not only possible to detect Zn^{2+} cations and F^- anions, but it can also distinguish between these two ions.

Among the various transition metal ions, zinc is the second most abundant transition metal in the human body. It plays a versatile role in a number of biological processes such as in the regulation of metalloenzymes, DNA binding and/or recognition, structural cofactors, neural signal transmission, as a catalytic center in many other processes[19-21]. Many Zn^{2+} fluorescent probes have been reported, which exhibited selectivity and sensitivity over other biologically essential metal ions over specific concentration ranges[22-24]. Although there are many Zn^{2+} probes, they are mostly for single target detection, and it is still a challenge to develop difunctional and multi-analyte responsive probes.

On the other hand, anions are ubiquitous and have major roles in a wide range of chemical, biological and environmental processes. The importance of anions has led to ongoing efforts in the development of sensors capable of selective recognition and sensing of anions[25-30]. Among these efforts, fluoride recognition has attracted substantial interest not only because of its unique properties but also its importance in our daily life[31-36]. Thus, the sensing of F^- has become a major focus and some excellent progress has recently been published[37-40]. In this paper, a difunctional probe **1** is reported which possesses the ability to detect and distinguish Zn^{2+} and F^-.

1 Experimental

1.1 Materials and methods

Unless otherwise stated, all reagents used were purchased from commercial sources and were used without further purification. 8-Formyl-7-hydroxycoumarin was prepared following the reported procedure[41]. The solutions of the metal ions were prepared from their nitrate salts (Aldrich and Alfa Aesar Chemical Co., Ltd.). All the anions used were tetra-n-butylammonium salts (Sigma-Aldrich Chemical Co.), and were stored in a desiccator under vacuum containing self-indicating silica. Other chemicals used in this work were of analytical grade and were used without further purification. Double distilled water was used throughout. Fluorescence spectral measurements were performed on a Cary Eclipse fluorescence spectrophotometer (Varian) equipped with a xenon discharge lamp using a 1 cm quartz cell. UV-Vis spectra were recorded on a UV-1800 spectrophotometer (Beijing General Instrument Co., China). IR spectra were obtained using a Vertex 70 FT-IR spectrometer (Bruker). ^1H and ^{13}C NMR spectra were measured on a WNMR-I 500 MHz NMR spectrometer (Wuhan Institute of Physics and Mathematics, Chinese Academy of Sciences) or a Nova-400 NMR spectrometer (Varian) respectively at room temperature using TMS as an internal standard. ESI-MS spectra were recorded on a Q Exactive spectrometer (Thermo).

MALDI-TOF mass spectra were measured on a BIFLEX III ultra-high resolution Fourier transform ion cyclotron resonance (FT-ICR) mass spectrometer (Bruker) with α-cyano-4-hydroxycinnamic acid as matrix. Isothermal titration calorimetry experiments were performed using a Nano ITC (TA); Cell fluorescence imaging was performed using an IX-71 (Olympus) fluorescence inverted phase contrast microscope.

1.2 Synthesis of probe 1

A solution of 8-formyl-7-hydroxy-coumarin (600 mg, 3.16 mmol) in dry ethanol (70 mL) was added dropwise to a solution of carbohydrazide (140 mg, 1.58 mmol) in dry ethanol (50 mL). The mixture was heated at reflux for 24 h. The product was collected by filtration and recrystallized from chloroform/methanol (4∶1, *V*/*V*) and obtained as a milky solid (471 mg, 68.7 %). m.p.>300 ℃; IR (cm^{-1}): 3 466, 2 929, 2 073, 1 726, 1 610, 1 243, 842. ^1H NMR (500 MHz, DMF-d_7): δ 6.35 (d, 2 H, *J*=10 Hz), 6.98 (d, 2 H, *J*=10 Hz), 7.70 (d, 2 H, *J*=10 Hz), 8.07 (d, 2 H, *J*=10 Hz), 8.99 (s, 2 H), 11.54 (s, 2 H) and 12.14 (s, 12.14); ^{13}C NMR (DMF-d_7): δ 162.1, 160.7, 154.5, 152.4, 145.8, 141.1, 131.7, 114.8, 113.1, 112.5 and 107.4; HRMS (ESI/TOF-Q) *m*/*z*: $[M+H]^+$ Calcd. for $C_{21}H_{15}N_4O_7$ 435.094 07; Found 435.093 72.

1.3 Spectral measurements

To a 10 mL volumetric flask containing different amounts of ions, the appropriate amounts of the solution of probe **1** were added directly with a micropipette, for Zn^{2+}, then diluted with DMF/H_2O (2∶3, *V*/*V*) mixed solvent to 10 mL; for F^-, diluted with DMF to 10 mL, then the fluorescence and absorption sensing of the ions was conducted. The fluorescence and UV-Vis spectra were measured after addition of ions at room temperature to equilibrium. Fluorescence measurements were carried out with an excitation and emission slit width of 10 nm.

1.4 Isothermal titration calorimetry determination (ITC)

The ITC experiment consisted of 35 consecutive injections, each at intervals of 240 s of 7 μL of ion solution (Zn^{2+} and F^- 1 mmol·L^{-1}) into the micro calorimetric reaction cell (1 mL) charged with a solution of probe **1** (0.1 mmol·L^{-1}) at 293.15 K with a stirring rate of 300 r·min^{-1}. DMF solvent was added to the reference cell as a thermal equilibrium reference. The heat of reaction was corrected for the heat of dilution of the ion solution determined in separate experiments. All solutions were degassed prior to the titration experiments by sonication. Computer simulations (curve fitting) were performed using the Nano ITC analyze software.

1.5 Cell culture and fluorescence imaging

PC3 cells were grown using a Roswell Park Memorial Institute-1640 supplemented with 10% fetal bovine serum, 100 U·mL^{-1} penicillin and 100 μg·mL^{-1} streptomycin at 37 ℃ and 5% CO_2 (*V*/*V*). One day prior to imaging, the cells were seeded in 6-well flat-bottomed plates. The next day, the cells were incubated with 10 μmol·L^{-1} of probe **1** for 30 min at 37 ℃. Before incubating with 50 μmol·L^{-1} $Zn(NO_3)_2$ for another 30 min, the cells were rinsed with fresh culture medium three times to remove the remaining sensor, then the fluorescence imaging of intracellular Zn^{2+} was observed under an inverted fluorescence microscope excited with UV light. The fluorescence imaging was observed after treatment of the cells with metal ion chelator, either 100 μmol·L^{-1} TPEN or 70 μmol·L^{-1} EDTA for 45 min. The cells which only incubated with 10 μmol·L^{-1} of probe **1** for 30 min act as a blank control.

2 Results and discussion

2.1 Synthesis

Probe **1** was obtained by the convenient condensation reaction of 8-formyl-7-hydroxy-coumarin and carbonic dihydrazide in a one-step process (Scheme 1). Its structure was elucidated by IR, ^1H NMR, ^{13}C NMR spectroscopy and mass spectrometry. The proton signal of the precursor aldehyde group had disapp-

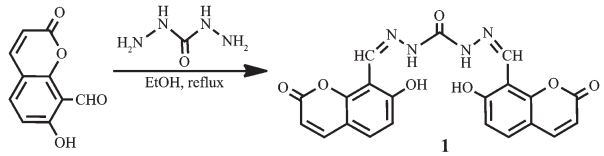

1

Scheme 1　Synthetic route for probe **1**

eared, whilst a new singlet appeared at about 8.99, which was attributed to the CH=N protons of the Schiff base skeleton (for details, see the Supporting Information, Fig.S1~S3).

2.2 Optical response of probe 1 to Zn^{2+}

Fluorescence and UV-Vis absorption spectroscopy were employed herein to investigate the recognition properties of probe **1**. In DMF/H_2O (2:3, *V*/*V*) solution, among the various tested metal cations Li^+, Na^+, K^+, Ag^+, Zn^{2+}, Mg^{2+}, Ca^{2+}, Ba^{2+}, Sr^{2+}, Hg^{2+}, Co^{2+}, Ni^{2+}, Cu^{2+}, Pb^{2+}, Cd^{2+}, Al^{3+}, Cr^{3+} and Fe^{3+}, probe **1** exhibited highly selective fluorescence enhancement in the presence of Zn^{2+} (the quantum yield Φ=0.38 vs quinine sulfate as reference material, Φ=0.56), whilst no significant fluorescence intensity changes were observed in the presence of any of the other metal ions (Fig.1a). The fluorescence intensity of probe **1**-Zn^{2+} were not affected when 90% volume fractions of water were added to the solution in DMF (Fig.S5). The fluorescence enhancement of probe **1** in the presence of Zn^{2+} could be ascribed to the formation of a chelate complex (rigid system) between probe **1** and the Zn^{2+} ion, leading to the chelation-enhanced fluorescence (CHEF) effect[18]. Meanwhile, the chelate effect also resulting in the inhibition of the C=N isomerization process and decreased non-radiative decay of the excited-state[42]. Fluorescence titration experiments revealed the detail complexation information for the process of probe **1** complexed with the Zn^{2+} (Fig.1b). As expected, when the concentration of Zn^{2+} was gradually increased from 0 to 4 equiv., the corresponding fluorescence intensity of probe **1** was gradually enhanced. The complex reached equilibrium with 1 equiv. Zn^{2+}, as shown in the inset. The 1:1 complex stoichiometry was further confirmed by a Job plot (Fig.1b, inset).

Interestingly, the UV-Vis absorption spectra of probe **1** exhibited a more remarkable phenomenon for the Zn^{2+} recognition. A dramatic red-shift (shifted from 310 to 360 nm) was observed in the presence of Zn^{2+} without any interference. It strongly suggested that Zn^{2+} ions can be readily and selectivity recognized by probe **1** (Fig.2a). Additionally, we can directly distinguish Zn^{2+} ion from various cations by the naked eye based on obvious colour changes (from colorless to bright yellow (Fig.2a, inset). Furthermore, the UV-Vis absorption titration experiment revealed a ratiometric behaviour with the formation of a new band at 360 nm and a decrease in the absorption band at 310 nm upon addition of Zn^{2+} (Fig.2b); isosbestic points appear at 338 nm. It is well-known that ratiometric response probes are better than any of other type of probes given their built-in correction for environmental effects and self-correcting capability[43-44]. All of these results are clear evidence that probe **1** could serve as a probe for the detection of Zn^{2+}. Molar ratio

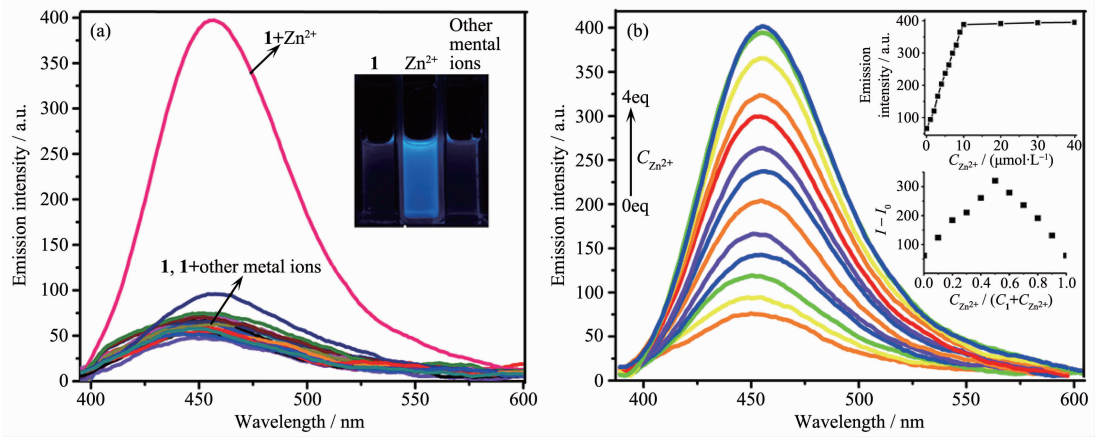

Inset in (a): colour change of probe **1** in the absence and the presence of Zn^{2+} under UV-Vis light; Inset in (b): variation of fluorescence intensity against the number of equivalents of Zn^{2+} and Job plot, λ_{ex}, λ_{em}=360, 454 nm

Fig.1 (a) Fluorescence spectra of probe **1** (10 μmol·L^{-1}, DMF/H_2O, 2:3, *V*/*V*) with 20 eq. of different metal ions; (b) Fluorescence spectral titration

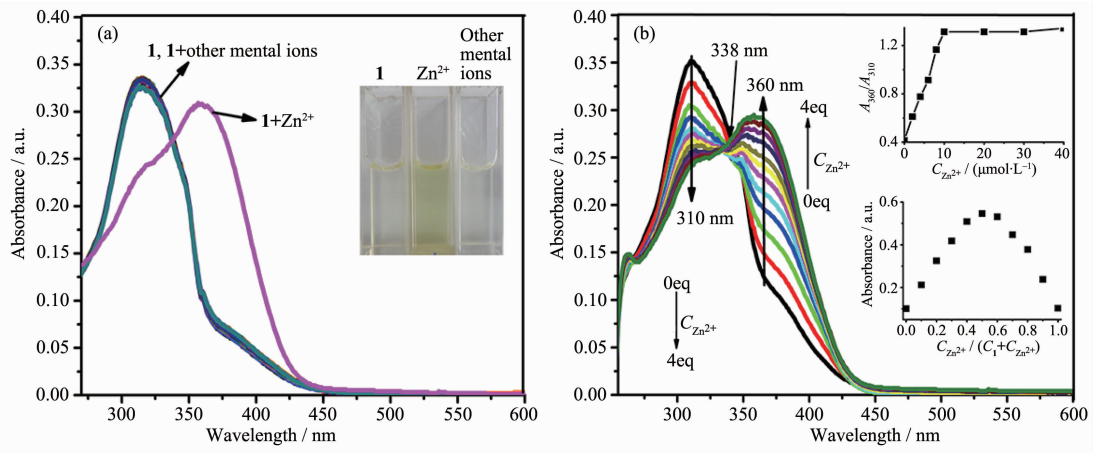

Inset in (a): colour change of probe **1** in the absence and the presence of Zn^{2+} under day light; Inset in (b): variation of ratio of absorbance against the number of equivalents of Zn^{2+} and Job plot, $A_{360\,nm}/A_{310\,nm}$

Fig.2　(a) Absorption spectra of probe **1** (10 μmol·L^{-1}, DMF/H_2O, 2:3, *V*/*V*) with 20 equiv. of different metal ions; (b) Absorption spectral titrations of probe **1** (10 μmol·L^{-1}, DMF/H_2O, 2:3, *V*/*V*) with Zn^{2+}

and Job plot analysis revealed a 1:1 stoichiometry (Fig. 2b, inset) for the complexation, which was further confirmed by MALDI-TOF mass spectrometry (Fig.S6). A mass peak at *m*/*z* 499.545 (Calcd. 499.409) was observed which corresponded to [**1**−2H+Zn+1]$^+$, strongly suggestive of the formation of a 1:1 complex, i.e. **1**-Zn^{2+}.

2.3　Optical response of probe 1 to F^-

In order to fully investigate the recognition properties of probe **1**, the interaction of probe **1** (10 μmol·L^{-1}) towards anions were also investigated by fluorescence and UV-Vis absorption spectroscopy in DMF solution. It was observed that there were no obvious changes in the fluorescence emission spectra upon addition of 20 equiv. of Cl^-, Br^-, I^-, NO_3^-, HSO_4^-, $H_2PO_4^-$, PF_6^- and ClO_4^- except for F^- (Fig.3a). The addition of F^- induced an acutely fluorescence enhancement (Φ=0.39 vs quinine sulfate as reference material, Φ=0.56) with a red shift from 440 to 475 nm which was attributed to the formation of a **1**-F^- complex. The colour of the solution changed from blue to a blue/green colour under ultraviolet light (Fig.3a, inset). Most noteworthy, a dramatic red-shift (from 310 to 400 nm) for F^- was observed in the UV-Vis absorption spectra (Fig.3b). Distinct colour changes (from colourless to deep yellow) were observed in the presence of F^-, and these could be visualized by the naked eye for detecting F^- vs the various other anions screened herein using probe **1** (Fig.3b, inset). These observations

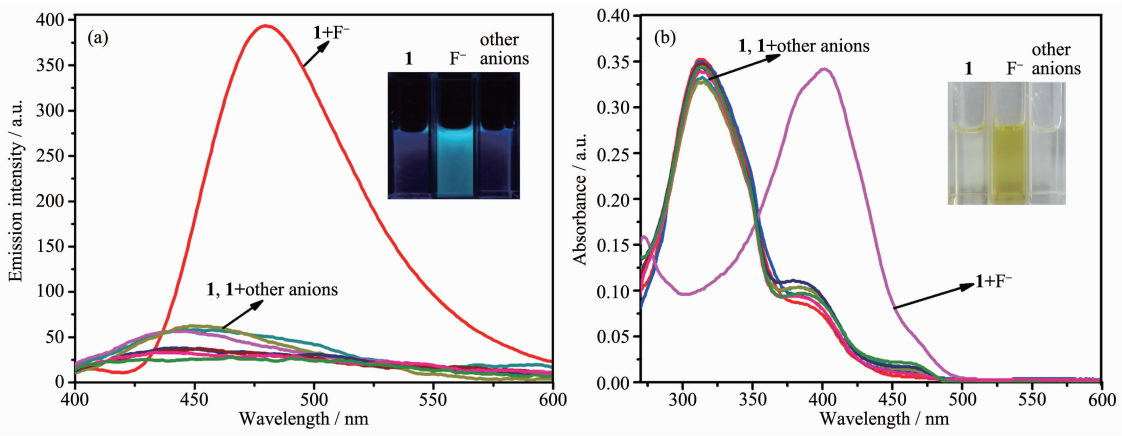

Inset: colour change of probe **1** in the absence and the presence of F^- under UV-Vis light (a), under day light (b); Anions: F^-, Cl^-, Br^-, I^-, NO_3^-, HSO_4^-, $H_2PO_4^-$, PF_6^-, ClO_4^-; λ_{ex}=400 nm

Fig.3　Fluorescence (a) and absorption (b) spectra of probe **1** (10 μmol·L^{-1}, DMF) with different anions (200 μmol·L^{-1})

strongly suggested that probe **1** is also an excellent probe for the detection of F^-.

In order to obtain more detailed complexation information for probe **1** with F^-, fluorescence and UV-Vis absorption titration experiments were also carried out. As expected, when the concentration of F^- was gradually increased from 0 to 4 equiv., the fluorescence intensity of probe **1** was gradually enhanced by about 7.4-fold in the fluorescence spectra (Fig.4a). On the other hand, the UV-Vis absorption titration experiments revealed a ratiometric behaviour with the formation of a new band at 400 nm for F^-, and a decrease in the absorption band at 310 nm upon addition of F^- (Fig.4b). This was also attributed to the formation of multiple hydrogen bonding involving the two phenolic-OH groups and two amide-NH groups. This binding interaction locks the C=N bond of **1** in place preventing its rapid isomerization and switching the fluorescence "on" which also seems to affect the intramolecular charge transfer (ICT) within the probe resulting in a red shift and a fluorescence colour change from non-fluorescence to blue/green. As mentioned previously, the unique ratiometric behaviour ($A_{310\ nm}/A_{400\ nm}$ for **1**-F^-), can provide a built-in correction for the environmental effect. Hence, probe **1** can also act as an excellent ratiometric probe for F^- due to the self-correcting capability. A 1:1 stoichiometry was confirmed by molar ratio and Job plot (Fig.4, inset).

Additionally, isothermal titration calorimetry (ITC) was employed here as it is a useful method for monitoring host-guest interactions[45-47]. In contrast to the experimental conditions for the preparation of cations/receptors complexes, ITC can still provide useful information on the interaction between guest cations and host receptors solutions. As shown in Fig. S7a, a representative titration curve can be obtained from an ITC experiment which revealed an abrupt transition point when the molar ratio of Zn^{2+} and probe **1** reached **1**, indicating the formation of a 1:1 complex of Zn^{2+} ion with probe **1**. Similar features were observed in the case of the **1**-F^- complex (Fig.S7b). Furthermore, the free energy $\Delta G^{\ominus}<0$ (−(95.68±2.13) kJ·mol^{-1} for **1**-Zn^{2+}complex and −(138.49±5.12) kJ·mol^{-1} for **1**-F^- complex) indicated that the binding processes are spontaneous. The stability constants (K_s) were determined to be (1.19±0.03)×10^4 L·mol^{-1} for **1**-Zn^{2+} and (5.24±0.04)×10^4 L·mol^{-1} for **1**-F^- by using the ITC method, respectively (Table 1). All of these results are

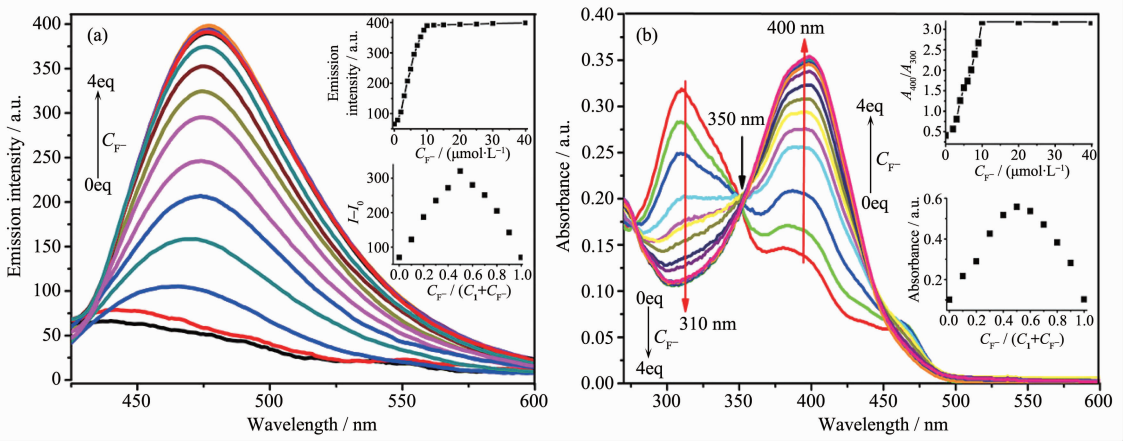

Inset: variation of fluorescence intensity (a) and ratio of absorbance (b) against the number of equivalents of F^- and Job plot; λ_{ex}, λ_{em}=400, 475 nm; $A_{400\ nm}/A_{310\ nm}$

Fig.4 Fluorescence (a) and absorption (b) spectral titrations of **1** (10 μmol·L^{-1}, DMF) with F^-

Table 1 Complex stability constant (K_s), enthalpy ($\Delta H^{\ominus}$) and entropy change ($T\Delta S^{\ominus}$) for the complexation of probe 1 with Zn^{2+} and F^- in DMF solution at 293.15 K

Complex	n	K_s / (L·mol^{-1})	$\Delta H^{\ominus}$ / (kJ·mol^{-1})	$\Delta S^{\ominus}$ /(J·mol^{-1}·K^{-1})
1-Zn^{2+}	1.00±0.024	(1.19±0.03)×10^4	−36.10±2.11	220.3
1-F^-	1.28±0.021	(5.24±0.04)×10^4	−54.41±3.21	275.9

Table 2　Analysis parameters for 1 and detection of Zn^{2+} and F^-

Method	Linear range of the calibration curve / (μmol·L^{-1})	Correlation coefficient	Limits of detection / (mol·L^{-1})
Fluorescence	0.1~12 (Zn^{2+})	0.997 3 (n=11)	3.4×10^{-8}
	0.1~11 (F^-)	0.980 9 (n=11)	2.9×10^{-8}
Absorption	0.2~12 (Zn^{2+})	0.992 5 (n=11)	1.6×10^{-7}
	0.4~10 (F^-)	0.985 0 (n=11)	3.6×10^{-7}

clear evidence that probe **1** is an excellent probe for both Zn^{2+} and F^- ions.

To further investigate the practical applicability of probe **1** (10 μmol·L^{-1}) as a Zn^{2+} ion selective fluorescent probe, competitive experiments were carried out in the presence of Zn^{2+} (20 eq.) mixed with Li^+, Na^+, K^+, Mg^{2+}, Ca^{2+}, Ba^{2+}, Sr^{2+}, Co^{2+}, Ni^{2+}, Pb^{2+}, Cd^{2+}, Ag^+, Hg^{2+}, Cu^{2+}, Fe^{3+}, Al^{3+} and Cr^{3+} (20 eq.) in DMF/H_2O (2:3, *V*/*V*) solution. As shown in Fig.S8, no significant interference to the selective response of probe **1** to Zn^{2+} was observed in the presence of any of the other metal ions employed herein when using either the UV-Vis and fluorescence method. Similarly, competitive anion experiments were also carried out in the presence of F^- mixed with 20 equiv. of coexisting anions Cl^-, Br^-, I^-, HSO_4^-, NO_3^-, ClO_4^-, PF_6^- and $H_2PO_4^-$ in DMF solution. As shown in Fig.S9, no obvious interference in the detection of F^- with probe **1** was observed in the presence of other competitive anions. Accordingly, these observations strongly suggested that probe **1** can be used as a selective probe for Zn^{2+} and F^- in the presence of the above mentioned ions for real life applications. Under the optimal conditions, the detection of linear relationships and limits of detection (LOD=3σ/slope) of probe **1** for Zn^{2+} and F^- are summarized in Table 2. The LOD of probe **1** towards the cation Zn^{2+}, and the anions F^- were of the order of 10^{-8} mol·L^{-1} by fluorescence or 10^{-7} mol·L^{-1} by the colorimetric method, which are far below most previously reported systems (Table S1)[14,37,48-52].

2.4　Cell imaging study

The capability of probe **1** to detect Zn^{2+} within living cells was investigated by fluorescence imaging on a fluorescence microscope, and the optical window at the blue channel was chosen as a signal output. Incubation of PC3 cells with 10 μmol·L^{-1} of probe **1** for 30 min at 37 ℃ gave almost no intracellular fluorescence as monitored in the bright-field image (Fig.5a and 5e) and in the fluorescence image (Fig.5b and 5f) by fluorescence microscopy. The incubated cells were then treated with 50 μmol·L^{-1} of Zn^{2+} for 30 min, whereupon a remarkable intracellular blue

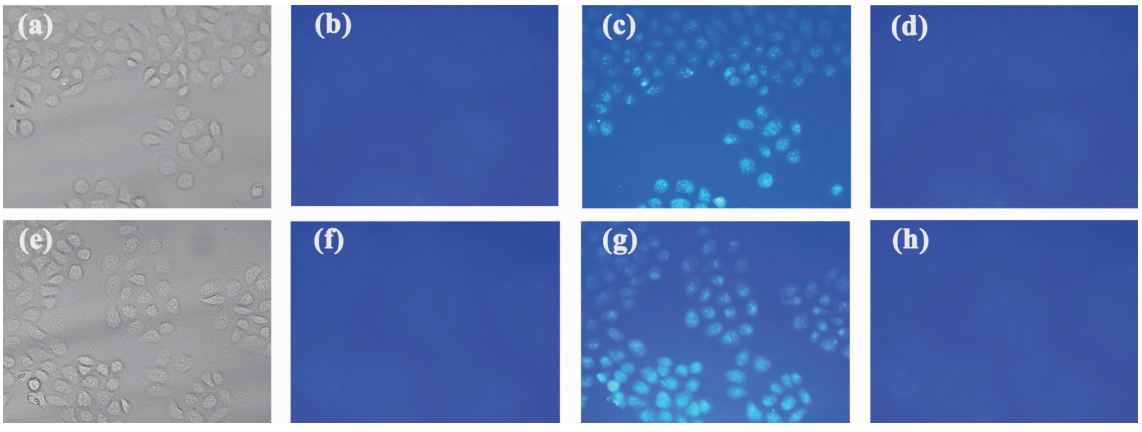

Fig.5　Fluorescence images of PC3 cells: (a) and (e) bright-field image of cells after incubation with probe **1** (10 μmol·L^{-1}); (b) fluorescence image of (a); (f) fluorescence image of (e); (c) and (g) blue fluorescence image of probe **1** (10 μmol·L^{-1}) treated cells after incubation with Zn^{2+} (50 μmol·L^{-1}) solution; (d) fluorescence image of probe **1** and Zn^{2+} solution treated cells which are the same as (c) after further incubation with TPEN (100 μmol·L^{-1}); (h) fluorescence image of probe **1** and Zn^{2+} solution treated cells which are the same as (g) after further incubation with EDTA (70 μmol·L^{-1})

fluorescence was observed (Fig.5c and 5g). However, the blue fluorescence can be quenched in the presence of membrane permeable Zn^{2+} chelators, such as, 100 μmol·L^{-1} TPEN (Fig.5d) or 70 μmol·L^{-1} EDTA (Fig. 5h) over 45 min. This "on-off" fluorescence behaviour in living cells was attributed to the strong scavenging action of TPEN (or EDTA) toward Zn^{2+}. It unambiguously confirmed that the blue fluorescence was induced by the response of probe **1** towards intracellular Zn^{2+}. This result suggested that probe **1** can penetrate the cell membrane in a short time and can monitor intracellular Zn^{2+} in PC3 cells by in vitro imaging and also potentially by in vivo methods.

Unfortunately, similar methods were unsuccessful when applied to the monitoring of F^- anions in living cells due to the presence of water, which resulted acute florescence quenching for the **1**-F^- complex.

2.5 Recognition mechanism of probe 1 towards ions

To further understand the recognition mechanism between probe **1** and Zn^{2+}, ^{1}H NMR titration studies were initiated in DMF-d_7 (Fig.6). When the concentration of Zn^{2+} was gradually increased, the proton signal of the hydroxyl group (O*H*, H_f) disappeared which may be attributed to deprotonation of the hydroxyl forming $O^-\cdots Zn^{2+}\cdots O^-$ interactions for complexation. Whilst the gradually lower field shift and broadening of the amide proton signal (N*H*, H_g) indicated that the amide group was affected by the complexation with Zn^{2+}. In other words, the amide moiety surrounds the Zn^{2+} to assistant the complexation process. However, there was no appreciable proton signal change for the coumarin moieties and the -N=CH protons (H_a~H_e). Thus, we propose the possible binding model for **1**-Zn^{2+} as shown in Scheme 2.

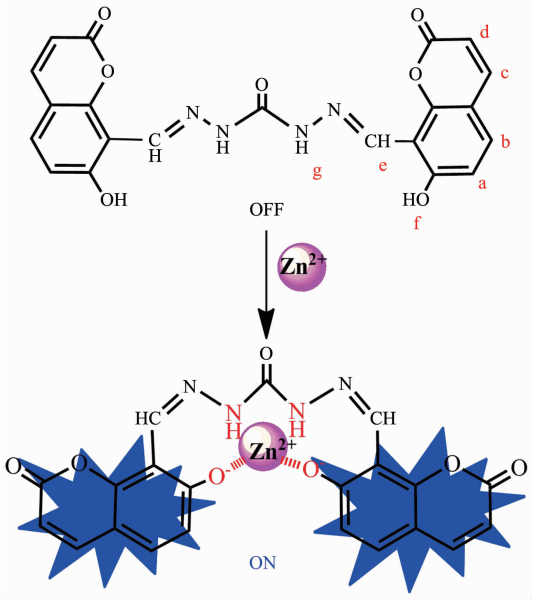

Scheme 2 Plausible binding model for the **1**-Zn^{2+} complex

^{1}H NMR titrations experiments were also carried out to investigate the F^- anion binding properties of probe **1** in DMSO-d_6. The signal of proton of hydroxyl (H_f, 11.98) and the amide NH proton (H_g, 11.12) of probe **1** disappeared when only 0.25 equiv. of F^- was added to the solution (Fig.7). However, no characteristic peak was observed in the region of ~16.0 due to the formation of an H-F^- complex even on increasing the addition of 2.0 equiv. of F^- [53-55]. These observations suggested that probe **1** complexed with F^- through multiple hydrogen bonds to form a host-guest complex without any deprotonation events. Simultaneously, the

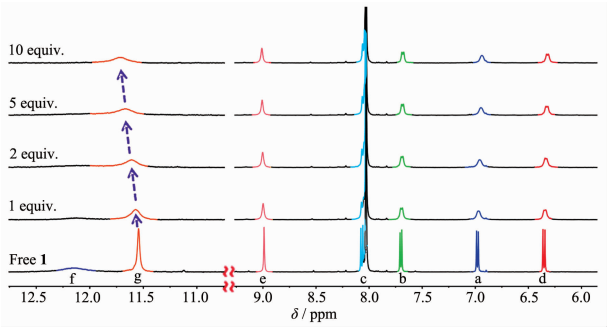

Fig.6 Partial ^{1}H NMR spectra of probe **1** (5.0 mmol·L^{-1}) and increasing concentrations of Zn^{2+} in DMF-d_7 at 298 K

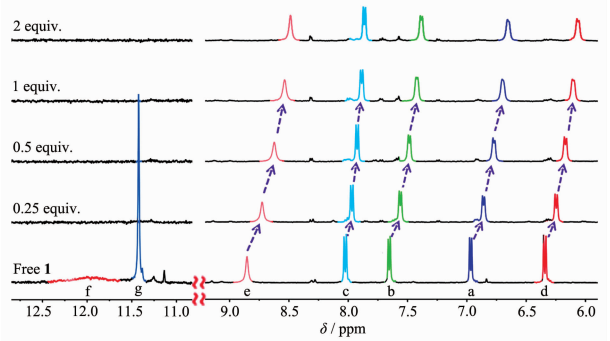

Fig.7 Partial ^{1}H NMR spectra of probe **1** (5.0 mmol·L^{-1}) and increasing concentrations of F^- in DMSO-d_6 at 298 K

-N=CH proton (H_e) and all the aromatic protons of the coumarine moieties (H_a, H_b, H_c, H_d) exhibited a progressive upfield shift which may be attributed to the π-π stacking between two coumarine which induced a shielding effect (Fig.7). Thus, we propose the possible anion complexation mode for probe **1** as shown in Scheme 3.

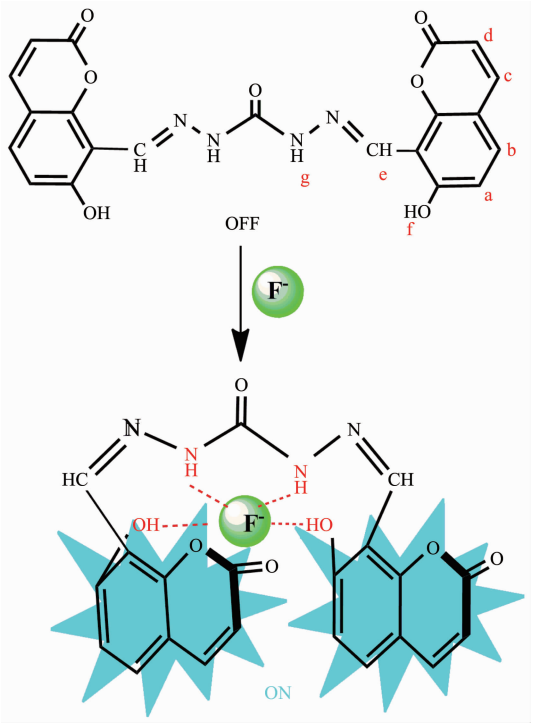

Scheme 3　Plausible binding model for the **1**-F^- complex

3　Conclusions

In summary, a fluorescent and ratiometric colorimetric probe **1** for Zn^{2+} and F^- has been readily prepared in a one-step procedure. Probe **1** exhibits high sensitivity and selectivity for Zn^{2+} and F^- through a "turn-on" fluorescence response over a range of other tested metal ions or anions with detection limits as low as 3.4×10^{-8} mol·L^{-1} and 2.9×10^{-8} mol·L^{-1}, respectively. Additionally, it also possesses excellent ratiometric behaviour towards Zn^{2+} and F^- which enables **1** to serve as a ratiometric probe. Moreover, we can easily distinguish the cation Zn^{2+} and the anions F^- via their max wavelength in their UV-Vis spectra (360 nm for **1**-Zn^{2+} vs 400 nm for **1**-F^- complex) or their fluorescent spectra (λ_{ex}, λ_{em}=360, 454 nm for **1**-Zn^{2+} vs λ_{ex}, λ_{em}=400, 475 nm for **1**-F^- complex) which are attributed to the different red-shifts. The mechanism of complexation behavior was fully investigated by UV-Vis and fluorescent spectral titrations, isothermal titration calorimetry, ^{1}H NMR spectroscopic titrations and mass spectrometry. Furthermore, the utility of probe **1** as a biosensor in living cells (PC3 cells) towards Zn^{2+} ions have been demonstrated. This work provides a promising strategy for the detection of metal ion and anionic species in biological and environmentally relevant systems.

Supporting information is available at http://www.wjhxxb.cn

References:

[1] Sun W, Guo S G, Hu C, et al. *Chem. Rev.*, **2016**,**116**:7768-7817

[2] Chen Y J, Yang S C, Tsai C C, et al. *Asian J. Chem.*, **2015**, **10**:1025-1034

[3] Samanta S, Datta B K, Boral M, et al. *Analyst*, **2016**,**141**: 4388-4393

[4] Sui H, Wang Y, Yu Z, et al. *Talanta*, **2016**,**159**:208-214

[5] Karakus E, Ucuncu M, Emrullahoglu M. *Anal. Chem.*, **2016**, **88**:1039-1043

[6] Zhou Z J, Xiao L, Xiang Y, et al. *Anal Chim. Acta*, **2015**, **889**:179-186

[7] Galbraith E, James T D. *Chem. Soc. Rev.*, **2010**,**39**:3831-3842

[8] Du J J, Hu M M, Fan J L, et al. *Chem. Soc. Rev.*, **2012**,**41**: 4511-4535

[9] Saleem M, Lee K H. *RSC Adv.*, **2015**,**5**:72150-72287

[10]You G R, Park G J, Lee S A. *Sens. Actuators B*, **2014**,**202**: 645-655

[11]Zhu H, Fan J L, Wang B. *Chem. Soc. Rev.*, **2015**,**44**:4337-4366

[12]Santos F, Luis E, Moragues M E, et al. *Chem. Soc. Rev.*, **2013**,**42**:3489-3613

[13]Ghosh T, Maiya B G, Samanta A. *Dalton Trans.*, **2006**,**6**:795-801

[14]Shellaiah M, Wu Y H, Lin H C. *Analyst*, **2013**,**138**:2931-2942

[15]Gonzalez M C, Oton F, Espinosa A. *Org. Biomol. Chem.*, **2015**,**13**:1429-1438

[16]Bhaumik C, Das S, Maity D. *Dalton Trans.*, **2011**,**40**:11795-11808

[17]Patil S R, Nandre J P, Jadhav D. *Dalton Trans.*, **2014**,**43**:

13299-13306

[18]Song E J, Kim H, Hwang I H. *Sens. Actuators B*, **2014**,**195**: 36-43

[19]Karak D, Das S, Lohar S. *Dalton Trans.*, **2013**,**2**:6708-6715

[20]Frederickson C J, Koh J Y, Bush A I. *Nat. Rev. Neurosci.*, **2005**,**6**:449-462

[21]Fraker P J, King L E. *Annu. Rev. Nutr.*, **2004**,**24**:277-298

[22]Chen H L, Guo Z F, Lu Z L. *Org. Lett.*, **2012**,**14**:5070-5073

[23]Jia J, Gu Z Y, Li R L, et al. *Eur. J. Org. Chem.*, **2011**:4609-4615

[24]Xue L, Li G P, Zhu D J, et al. *Inorg. Chem.*, **2012**,**51**:10842-10849

[25]Gale P A. *Chem. Soc. Rev.*, **2010**,**39**:3746-3771

[26]Caltagirone C, Gale P A. *Chem. Soc. Rev.*, **2009**,**38**:520-563

[27]Sessler J L, Gale P A, Cho W S. *Anion Receptor Chemistry*. Cambridge: RSC, **2006**:259

[28]Beer P D, Gale P A. *Angew. Chem. Int. Ed.*, **2001**,**40**:486-516

[29]Ghosh D, Rhodes S, Hawkins K. *New J. Chem.*, **2015**,**39**: 295-303

[30]Ashton T D, Jolliffe K A, Frederick M. *Chem. Soc. Rev.*, **2015**,**44**:4547-4595

[31]Dhillon A, Nair M, Kumar D. *Anal. Methods*, **2016**,**8**:5338-5352

[32]Arhima M H, Gulati O P, Sharma S C. *Phytother. Res.*, **2004**,**18**:244-246

[33]Matsui H, Morimoto M, Horimoto K. *Toxicol. in Vitro*, **2007**, **21**:1113-1120

[34]Horowitz H S. *J. Public Health Dent.*, **2003**,**63**:3-8

[35]Ayoob S, Gupta A K. *Crit. Rev. Environ. Sci. Technol.*, **2006**,**36**:433-487

[36]Bassin E, Wypij D, Davis R. *Cancer Causes Control*, **2006**, **17**:421-428

[37]Lee J J, Park G J, Choi Y W. *Sens. Actuators B*, **2015**,**207**: 123-132

[38]Rosen C B, Hansen D J, Kurt V. *Org. Biomol. Chem.*, **2013**, **11**:7916-7922

[39]Ahmed N, Suresh V, Shirinfar B. *Org. Biomol. Chem.*, **2012**, **10**:2094-2100

[40]You G R, Park G J, Lee S A. *Sens. Actuators B*, **2014**,**202**: 645-655

[41]Nelly N M, Shihab D D, Edikan E A. *J. Inclusion Phenom. Macrocyclic Chem.*, **2010**,**68**:305-312

[42]Wang L Y, Li H H, Cao D. *Sens. Actuators B*, **2013**,**181**: 749-755

[43]Zhao J L, Tomiyasu H, Wu C. *Tetrahedron*, **2015**,**71**:8521-8527

[44]Wu Y S, Li C Y, Li Y F. *Sens. Actuators B*, **2014**,**203**:712-718

[45]Grolier J P E, Río J M D. *J. Chem. Thermodyn.*, **2012**,**55**: 193-202

[46]Makowska J, Żamojć K, Wyrzykowski D. *Spectrochim. Acta Part A*, **2016**,**153**:451-456

[47]Freire E, Mayorga O L, Straume M. *Anal. Chem.*, **1990**,**62**: 950A-959A

[48]Orojloo M, Amani S. *Talanta*, **2016**,**159**:292-299

[49]Nayan R, Abhijit D, Paritosh M, et al. *Sens. Actuators B*, **2016**,**236**:719-731

[50]Das A K, Goswami S, Quah C K, et al. *RSC Adv.*, **2016**,**6** (22):18711-18717

[51]Nemati M, Hosseinzadeh R, Zadmard R, et al. *Sens. Actuators B*, **2017**,**241**:690-697

[52]Dhara A, Guchhait N, Mukherjee I, et al. *RSC Adv.*, **2016**, **6**:105930-105939

[53]Zhang Y P, Jiang S M. *Org. Biomol. Chem.*, **2012**,**10**:6973-6979

[54]Sharma D, Sahoo S K, Chaudhary S. *Analyst*, **2013**,**138**: 3646-3650

[55]Khanmohammadi H, Rezaeian K. *RSC Adv.*, **2014**,**4**:1032-1038